RAA 2018 Vol. **18** No. **2**, 17(10pp) doi: 10.1088/1674–4527/18/2/17

http://www.raa-journal.org *http://iopscience.iop.org/raa*

Research in Astronomy and Astrophysics

Statistical analysis of dynamic fibrils observed from NST/BBSO observations

Thambaje Gopalan Priya[1,2], Jiang-Tao Su[1,2], Jie Chen[1,3], Yuan-Yong Deng[1] and Debi Prasad Choudhury[4]

[1] Key Laboratory of Solar Activity, National Astronomical Observatories, Chinese Academy of Sciences, Beijing 100012, China; *priyatg@nao.cas.cn*

[2] University of Chinese Academy of Sciences, Beijing 100049, China

[3] State Key Laboratory for Space Weather, Center for Space Science and Applied Research, Chinese Academy of Sciences, Beijing 100190, China

[4] California State University, Northridge, CA 91330, USA

Received 2017 October 11; accepted 2017 November 14

Abstract We present the results obtained from the analysis of dynamic fibrils in NOAA active region (AR) 12132, using high resolution Hα observations from the New Solar Telescope operating at Big Bear Solar Observatory. The dynamic fibrils are seen to be moving up and down, and most of these dynamic fibrils are periodic and have a jet-like appearance. We found from our observations that the fibrils follow almost perfect parabolic paths in many cases. A statistical analysis on the properties of the parabolic paths showing an analysis on deceleration, maximum velocity, duration and kinetic energy of these fibrils is presented here. We found the average maximum velocity to be around 15 km s^{-1} and mean deceleration to be around 100 m s^{-2}. The observed deceleration appears to be a fraction of gravity of the Sun and is not compatible with the path of ballistic motion due to gravity of the Sun. We found a positive correlation between deceleration and maximum velocity. This correlation is consistent with simulations done earlier on magnetoacoustic shock waves propagating upward.

Key words: Sun: sunspots-oscillation — Sun: magnetic fields — Sun: chromosphere

1 INTRODUCTION

The chromosphere that lies between the photosphere and the hot corona often reveals jet-like features, which are small in size and have very short lifetimes. Though there has been a lot of confusion about the relationship between the quiet Sun limb spicules, mottles observed on the quiet sundisk and dynamic fibrils (DFs) (Grossmann-Doerth & Schmidt 1992), these three phenomena are related (Tsiropoula et al. 1994). The physical processes that occur in the chromosphere are not well understood, especially mass and energy transportation in DFs (see Rutten 2012). The flows (up and down) from photosphere to chromosphere and the higher-layer corona exhibit a variety of oscillation modes like three-minute, five-minute and seven-minute oscillations. Tian et al. (2014) first presented strong evidence related to the shock behavior of sunspot oscillations in the transition region (TR) and in the chromosphere based on IRIS observations. The 5-minute oscillations (Leighton et al. 1962) happening over these sunspots have been studied extensively over a period of time and it has been found that there is a decrease in amplitude with height that is not easily detected in higher layers above the photosphere. The 3-minute oscillations could be due to the mode conversion of magnetoacoustic waves (Stangalini et al. 2012). The fibrilar structure of the chromosphere reveals that magnetic fields play a significant role (Hale 1908). The jet-like features which are also known as spicules, mottles and DFs are observed on the limb, quiet Sun disk and in active regions (ARs) respectively. Our main concentration is about observations of DFs. The dynamics of DFs and their imprint on TR, as well as their oscillations, have been extensively studied (de Pontieu et al. 1999; De Pontieu et al. 2003a,b, 2004). The remarkable power of oscillations in the DFs was determined by De Pontieu et al. (2003a). This was discovered using high resolution data from the Swedish 1-m Solar Telescope (SST). De Pontieu et al. (2004) and de Pontieu & Erdélyi (2006) constructed a model which explains the reason for DFs to be the inclination of magnetic field lines. This inclination reduces acoustic cut off frequency permitting a longer period, so called p-mode waves to leak into the atmosphere where they form shocks and these shocks are the mechanism driving the DFs. This was further investigated and demonstrated by Hansteen et al. (2006) using similar data from SST that the DFs are caused by magnetoacoustic shock waves. In this paper we analyzed the motion of DFs using the New Solar Telescope (NST, Cao et al. 2010) (now known as the Goode Solar Telescope (GST), after July 2017) operating at Big Bear Solar Observatory (BBSO) by measuring its properties and describing its temporal evolution. Our results support the fact that the DFs are formed due to shock waves in the chromosphere that are driven by flows that are convective and photospheric oscillations as reported by De Pontieu et al. (2004). Through analysis of a dataset taken at NST, we find that the DFs and their properties could be a result of shock waves that are generated from the p-mode propagating upward.

2 OBSERVATIONS AND DATA PROCESSING

The sunspot of NOAA AR 12132, located at S09E08 on 2014 August 5 from BBSO (NST, Cao et al. 2010), was chosen for studying the DFs (see Fig. 1). The pointer was (270″, 395″), targeting the sunspot of AR 12132. The observations were performed using NST during 18:20 UT−19:20 UT. Chromospheric images were acquired every 23 s by scanning the Hα spectral line from the blue wing -1 Å to red wing +1 Å with a step of size 0.2 Å. The field of view is about 70″, and has a pixel scale of 0.029″ pixel^{-1}. The data are used to investigate the umbral oscillations in the chromospheric sunspot at different solar altitudes observed on August 5. A combination of a 5 Å interference filter and a Fabry-Perot etalon is used in the Visible Imaging Spectrometer (VIS) to get a bandpass of 0.07 Å at the Hα line. We chose the first Hα -1.0 Å image as a reference image to align all other images in this passband. The relative shifts were recorded, and used to register the images in the other passbands of Hα.

3 DATA ANALYSIS AND RESULTS

A close look at the movie of Hα line core images gives insight into fibrils located in the close proximity and in the vicinity of the sunspot near the image center, a few of which were colligated with the superpenumbra. We investigate 40 such DFs in this study, wherein most AR DFs from the line core of Hα images indicate almost a perfect parabolic path. We opt for choosing the direction of a DF, or a bunch of DFs, manually using CRisp SPectral EXplorer (CRISPEX,Vissers & Rouppe van der Voort 2012) which helps in analyzing the multidimensional data cubes and additional software called Timeslice ANAlysis tools (TANAT) for analyzing and also for various measurements of data. The comprehensive application of this software not only made viewing the sequence of images easier but also helped in tracking the events that were very clear while ascending and descending along their individual paths in 584 jet-like features in Hα. CRISPEX is a widget-based versatile IDL tool for visual inspection and analysis of high resolution data. CRISPEX also generates the space-time diagram for all linear as well as curved paths. This information can be stored and retrieved later for further analysis. We have produced the space-time diagram for all the 40 DFs detected. The space-time diagram for one of the DFs is shown in Figure 2 and its evolution is displayed in Figure 2. The figure illustrates the recession of the already risen DF along the same path. We have detected almost 584 such trajectories and applied a parabolic fitting to each trajectory.

Figure 4 displays an example of the fitting. From the fit, we calculate parameters like deceleration, maximum velocity, maximum height, duration and kinetic energy as well. We assume the electron density to be same throughout the chromosphere.

This electron density (n_e) multiplied by the mass of the electron (m_e) gives density ($\rho = n_\mathrm{e} m_\mathrm{e}$) which means that the kinetic energy per unit volume would be equal to the square of the maximum velocity (KE = v^2_max/2). The kinetic energy per unit volume of these jet-like features may transform further into heat and might play a significant role in heating the corona.

We obtained the maximum velocity is between $10\,\mathrm{km\,s^{-1}}$ and $30\,\mathrm{km\,s^{-1}}$ and deceleration is between

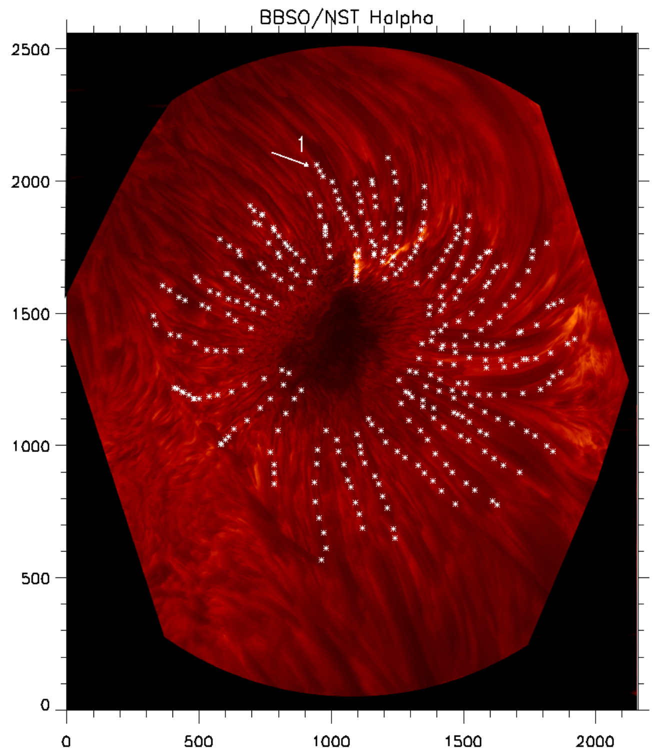

Fig. 1 Hα line core image showing the paths of DFs overplotted. The DF marked as '1' is used for further analysis. Tick marks are in pixels.

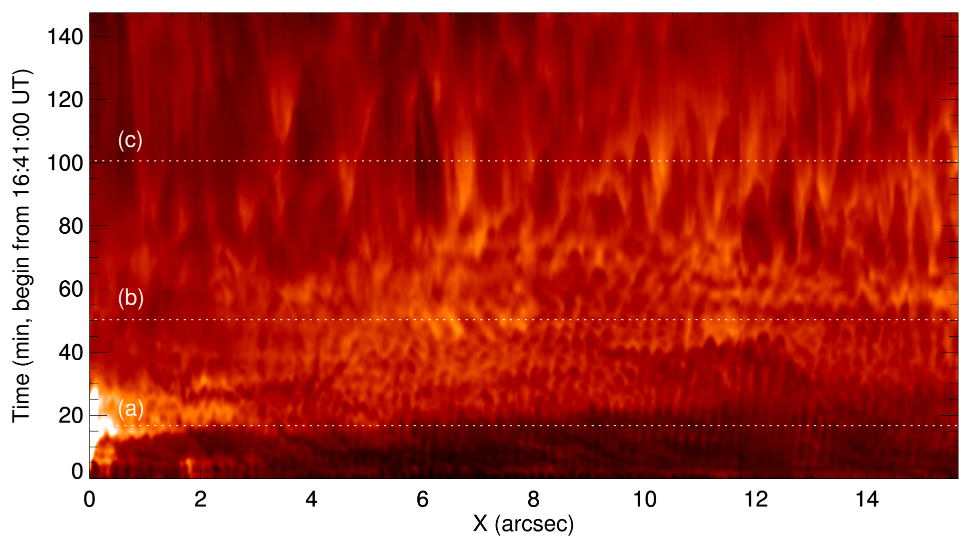

Fig. 2 Space-time diagram of the Hα line center image for DF marked as '1' in Fig. 1. The three dotted lines indicate the umbral (a), penumbral (b) and superpenumbral (c) regions for which the power spectra are shown in Fig. 7.

$50\,\mathrm{m\,s^{-2}}$ and $200\,\mathrm{m\,s^{-2}}$. We noticed that these correlations are quite similar to the measurements on DFs done by Hansteen et al. (2006). However, we found that the correlation between duration and deceleration/maximum velocity is comparatively weaker, showing a high scatter and nonlinearity in almost all the DFs.

As can be seen in De Pontieu et al. (2007), the correlation between duration and deceleration/maximum velocity is not so clear, or in other words weak. Similar results have been obtained by Langangen et al. (2008) in DFs with the reason being the effect of projection. It could be probable that there is no effect of projection

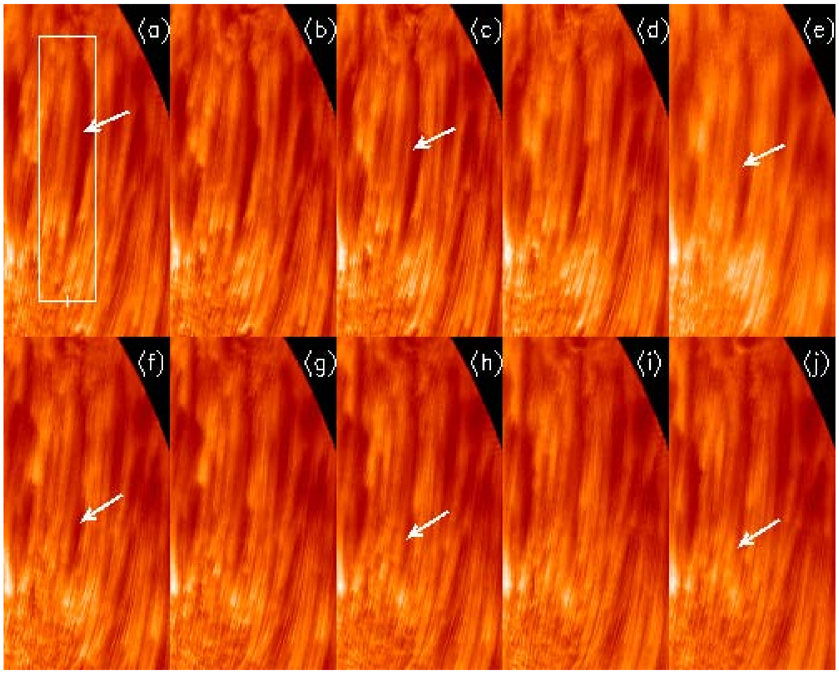

Fig. 3 Snapshots of the Hα line core showing the temporal evolution of DFs (marked as '1' in Fig. 1) as it recedes.

seen in duration whereas the effect is more prominent in velocity and deceleration. It is very clear from the scatter plots in Figure 5 that the correlation between duration and deceleration/maximum velocity is ambiguous with huge scatter and difference in slopes.

By tracing all the jet-like features, we generated the histograms of maximum velocity, duration, deceleration and kinetic energy, as shown in Figure 6. From the histograms, it can be ascertained that the maximum velocity, duration and deceleration follow Gaussian distributions. The maximum velocities are within $10\,\mathrm{km\,s^{-1}}$ to $30\,\mathrm{km\,s^{-1}}$ and the average is about $15\,\mathrm{km\,s^{-1}}$, the duration ranges from 2 min to 20 min and the average is about 11 min, and the deceleration ranges from $10\,\mathrm{m\,s^{-2}}$ to $200\,\mathrm{ms^{-2}}$ and the average is around $100\,\mathrm{m\,s^{-2}}$.

We obtain the average maximum height to be around 0.025 Mm. We find the kinetic energy of all the 584 jet-like features and estimate its average to be about $220\,\mathrm{gm\,cm^{-1}\,s^{-2}}$, and find that it follows a partial Gaussian distribution.

We take the Fourier power spectra along the DF (originating from the umbral boundary and propagating higher into the superpenumbral region) at three different points along the DF as shown in Figure 7. The power spectrum in Figure 7(a) is at the umbral boundary, that in (b) is at the penumbral region and that in (c) is at the superpenumbral region. The running waves travel through the boundary of the umbra and penumbra and eventually disappear at the penumbral boundary. In the power spectra we see oscillations in DF varying with time. To measure the oscillation period, we use the Fast Fourier Transform (FFT) function that is available in IDL.

As shown in Figure 7, the frequency at the umbral boundary is $\approx$4.3 mHz and based on the frequency of the power spectra, the oscillation period at the same point is 235 s. The results show that the oscillations within umbra are typical 3-min oscillations with period $T = 235\,\mathrm{s}$, and the corresponding oscillations within the penumbra are typical 5-min oscillations with period $T = 345\,\mathrm{s}$ and, $T = 408\,\mathrm{s}$. The period of umbral oscillations is almost half that of the penumbral oscillations. The corresponding periods of umbral and penumbral oscillations measured by applying the FFT function are $T_{\mathrm{umbra}} = 235\,\mathrm{s}$ and $T_{\mathrm{penumbra}} = 408\,\mathrm{s}$ respectively. These oscillations propagate higher up and further develop into shocks as shown in Figure 8, suggesting oscillations are upwardly propagating shock waves.

Each panel in Figure 8 corresponds to three different positions along the marked DF in Figure 1. It is quite possible that the DFs are usually driven in synchrony with the sunspot oscillations (Chae et al. 2014). The oscillations propagate higher and develop into shocks which propel the fibrils several times. Thus, we speculate that the shock driven DFs are related to sunspot oscillations.

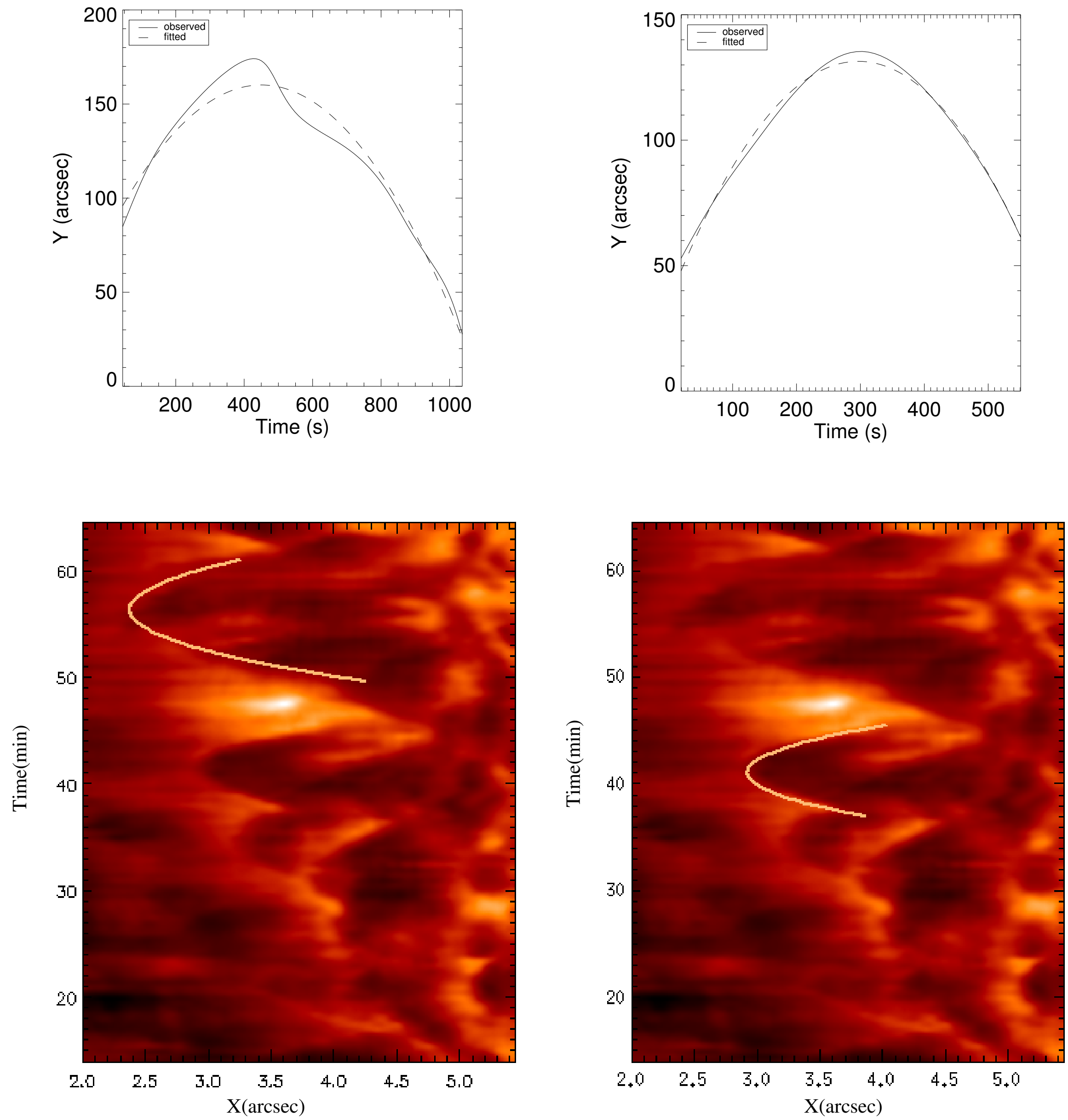

Fig. 4 The extracted portions of $x - t$ plots for sample DFs are shown in the bottom panels. The DFs follow almost a perfect parabolic path. The yellow lines indicate the best fit used to derive the deceleration, maximum velocity, duration and maximum height. The parabolic fittings for corresponding trajectories are shown in the top panels.

To be more precise, there exists a form of propagation of shock wave fronts that starts from the sunspot center and reaches the bottom of the fibrils, then propagates higher along the DF (Chae et al. 2014). Hence, it is clear that the DFs are physically related to the sunspot oscillations and the form of shock fronts that propagate from the sunspot center.

Figure 8 shows the temporal-spectral variations (t-λ plots), indicating the oscillations at three different positions along the DF (connecting the sunspot to the fibril), to in fact be the upwardly propagating shock waves. Hansteen et al. (2006) and De Pontieu et al. (2007) simulated upwardly propagating magnetoacoustic shock waves and were able to recreate the observed behavior of dynamic fibrils. They found that the highly dynamic chromospheric shock waves cause significant upward and downward motion of the upper chromosphere. The transition of an upwardly propagating shock through the chromosphere produces a sawtooth or N-shape form (as seen in Fig. 8), which indicates a blueshift followed

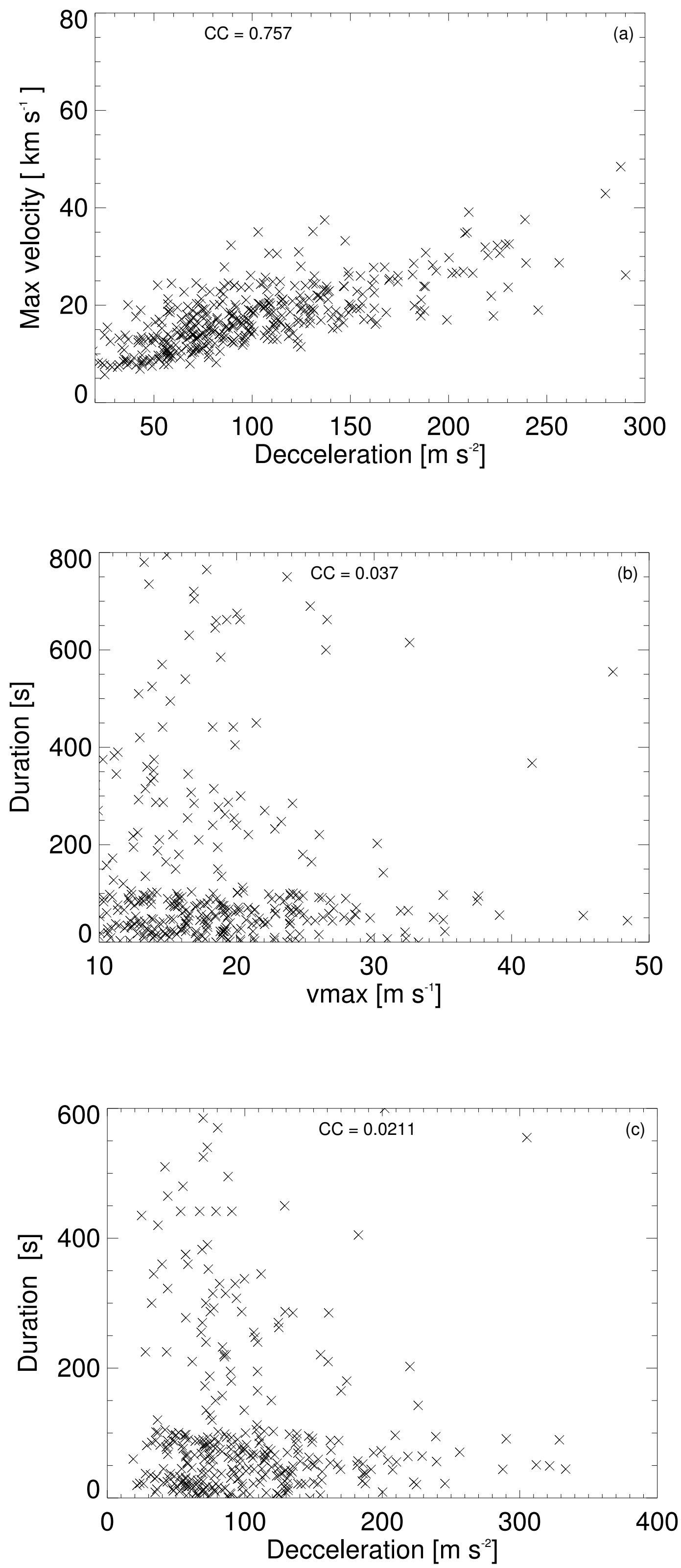

Fig. 5 (a) Scatter plots of deceleration vs. maximum velocity, (b) maximum velocity vs. duration, and (c) deceleration vs. duration. A clear linear correlation exists between deceleration and maximum velocity.

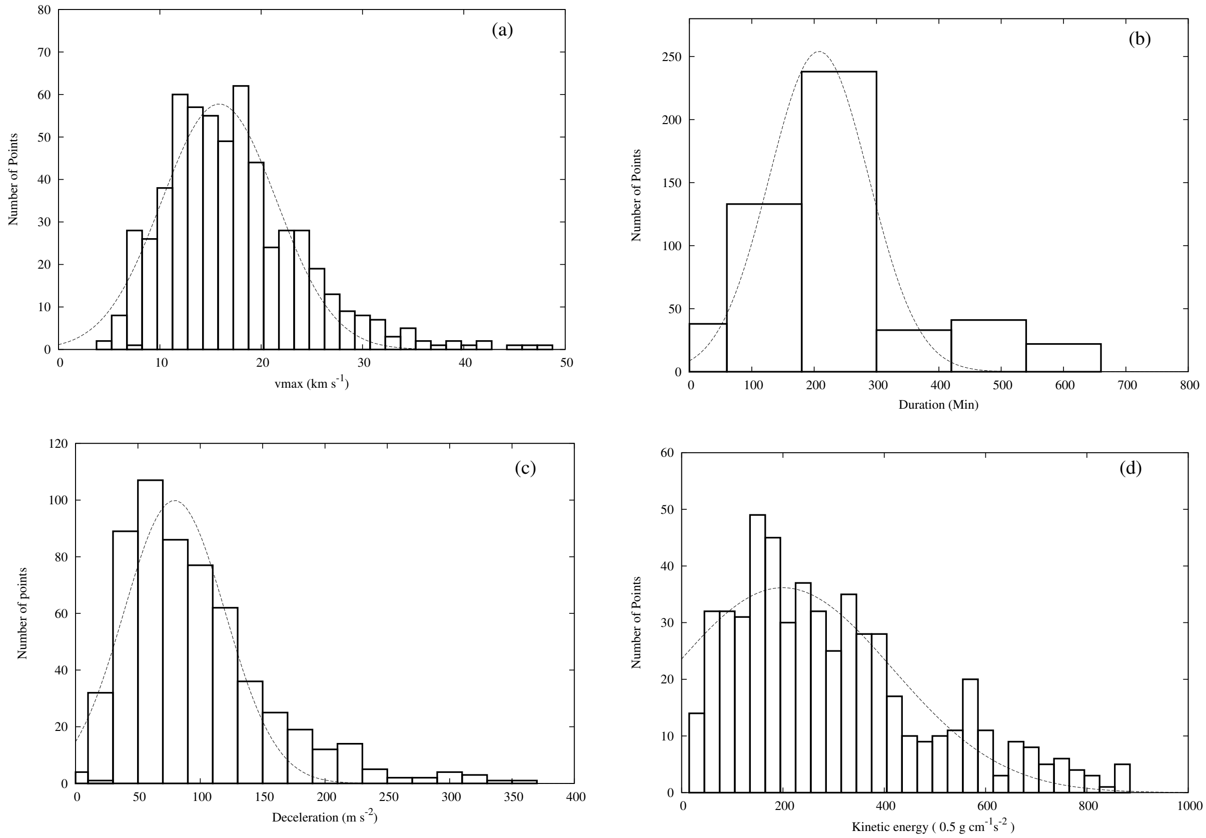

Fig. 6 Distributions of the maximum velocity (a), duration (b), deceleration (c) and kinetic energy (d). The histograms are constructed from the observations of DFs.

by a gradual drift towards the redshift and then a sudden appearance of a blueshift (Hansteen et al. 2006; Vecchio et al. 2009). The N-shape pattern preponderates in all the three t-λ plots constructed at different locations along the DF and hence confirms the idea of shock driven fibrils. The correlation coefficient between the maximum velocity and deceleration of a sample of 40 sunspot DFs is 0.757. This demonstrates that the oscillations in sunspots are the magnetoacoustic shock waves that propagate upward (e.g.,Lites 1986; Centeno et al. 2006; Chae et al. 2014; Tian et al. 2014; Yurchyshyn et al. 2014).

4 DISCUSSION AND CONCLUSIONS

The above identified correlations could probably be a significant signature for jets that are periodic, which are perhaps driven by waves that normally propagate from the photosphere into the chromosphere and hence steepen into shocks (Rouppe van der Voort & de la Cruz Rodríguez 2013). The maximum velocities of these jet-like features that we have located in our data are usually between $10-30\,\mathrm{km\,s^{-1}}$, and are found to be similar in comparison to Hansteen et al. (2006); De Pontieu et al. (2007). The chromospheric waves are usually created by normal convective flows and are also due to oscillations found in the photosphere and also in the convection zone. These disturbances further propagate upward into the chromosphere and thereby form shocks that become a driving force for the plasma in the chromospheric region, hence resulting in the formation of DFs. The periods that are longer than the period of local acoustic cut off are blocked by the chromosphere. This cut off period is completely dependent on the magnetic field line inclination with respect to the vertical (Suematsu 1990; De Pontieu et al. 2004). A single shock could possibly drive the DFs and is also, we believe, the reason for the correlation between deceleration and maximum velocity. These DFs are the direct consequence of upwardly propagating chromospheric oscillations/waves that are produced in the convection zone or photosphere as a result of global p-mode oscillations and also convective flows. These waves propagate into the chromosphere and pass through to the region where Hα is formed, thus thereby

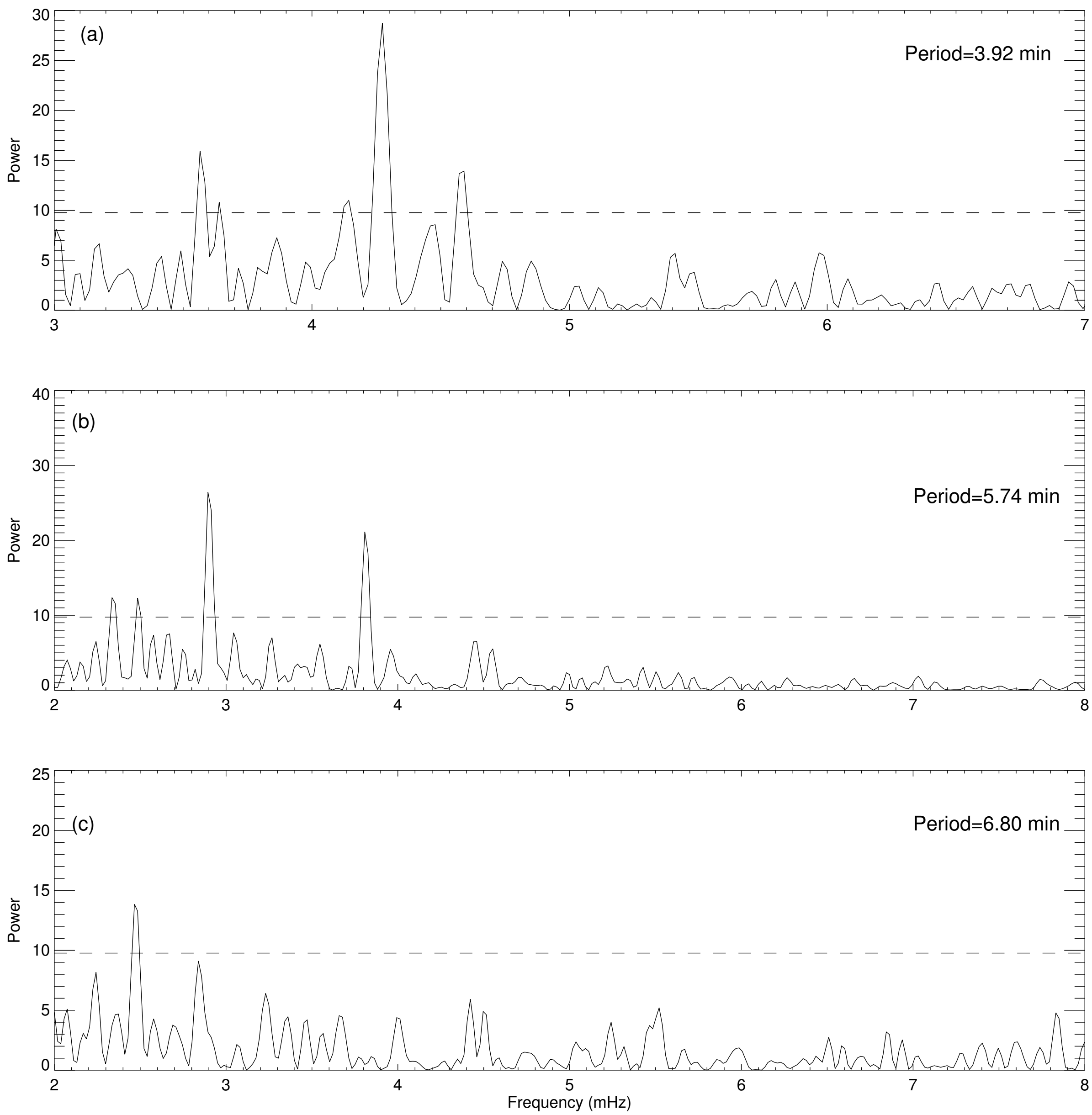

Fig. 7 The Fourier power spectra at positions marked in white dotted lines in Fig. 2.

generating shocks during its upward propagation. The fact on which we stress our interpretation is that the DFs follow a parabolic path with a good positive correlation between the properties like velocity and deceleration for all of the detected DFs. We found that velocity and deceleration are directly proportional to each other. The velocity that Suematsu et al. (1995) report for their event with mottles is in the range $10-30\,\mathrm{km\,s^{-1}}$ and we found it to be rather similar to what we identified in our BBSO/NST observations for our DF event. The same has been seen by Hansteen et al. (2006) and it is evident that the formation of DFs is due to shocks in the chromosphere driven by the photospheric convective flows as well as oscillations. Hence, we conclude that the driving mechanism is the same. Heggland et al. (2007) and Heggland et al. (2011) explain that the usually long period waves propagate into the solar atmosphere along the magnetic field lines which are inclined. The most essential conclusion is the explanation that the driving force for DFs is the so called magnetoacoustic shocks that are induced by the

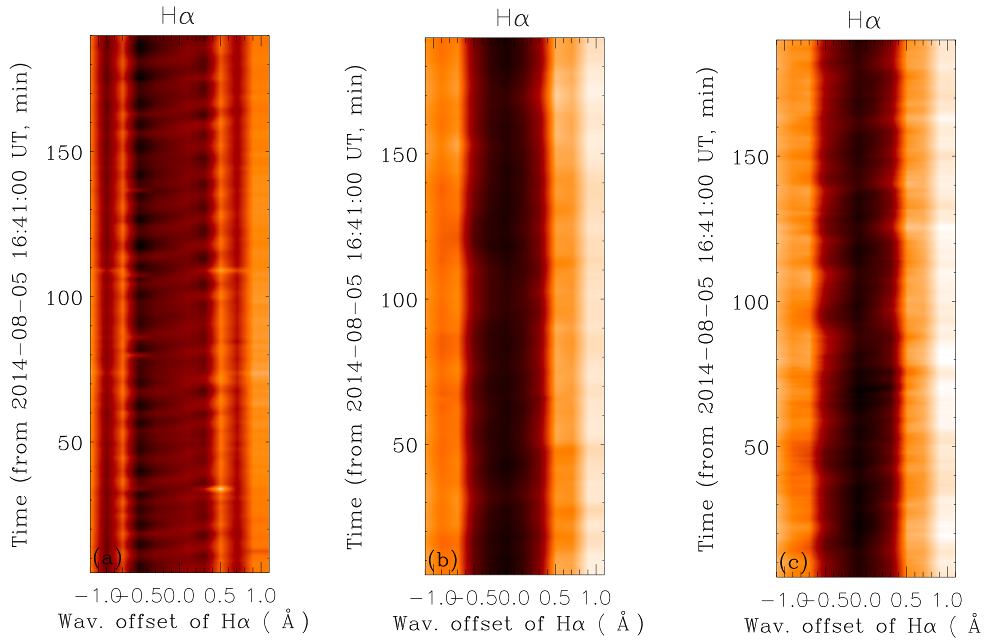

Fig. 8 Shock waves along the DFs. The wavelength-time maps of the Hα spectral line at different points along the DF as it propagates upwardly are shown in (a), (b) and (c).

p-mode oscillations in addition to leakage of convective flows into the chromosphere. Both observations (Lites 1992) and simulations (Bard & Carlsson 2010) provide enough evidence for waves that propagate upwards and also shocks in the atmosphere of sunspots. This phenomenon appears as a dark feature in Hα images and is due to the density of magnetic flux. De Pontieu et al. (2004) proposed that the similarity between observations and some modeling done earlier on DFs provides the reason for upward and downward movement of the upper chromosphere, which is due to shock waves in the chromosphere. Zhang et al. (2017) demonstrated that oscillations which appear to be like surge or light walls lying above light bridges are also caused by shocks. Our findings indicate that in ARs, most of these jet-like features are caused by shocks in the chromosphere.

Acknowledgements T.G.P would like to thank Patrick Antolin for his valuable help on CRISPEX. This work is supported by the National Natural Science Foundation of China (Grant Nos. 11427901, 11773038, 11373040, 11373044, 11273034, 11303048, 11178005 and 11711530206) and also supported partly by the State Key Laboratory for Space Weather, Center for Space Science and Applied Research, Chinese Academy of Sciences. BBSO operation is supported by NJIT, US NSF AGS-1250818 and NASA NNX13AG14G. T.G.P thanks financial support from the CAS-TWAS Presidents PhD fellowship – 2014. We thank the referee for review and for useful comments and suggestions.

References

Bard, S., & Carlsson, M. 2010, ApJ, 722, 888
Cao, W., Gorceix, N., Coulter, R., et al. 2010, Astronomische Nachrichten, 331, 636
Centeno, R., Collados, M., & Trujillo Bueno, J. 2006, ApJ, 640, 1153
Chae, J., Yang, H., Park, H., et al. 2014, ApJ, 789, 108
de Pontieu, B., Berger, T. E., Schrijver, C. J., & Title, A. M. 1999, Sol. Phys., 190, 419
de Pontieu, B., & Erdélyi, R. 2006, Philosophical Transactions of the Royal Society of London Series A, 364, 383
De Pontieu, B., Erdélyi, R., & de Wijn, A. G. 2003a, ApJ, 595, L63
De Pontieu, B., Tarbell, T., & Erdélyi, R. 2003b, ApJ, 590, 502
De Pontieu, B., Erdélyi, R., & James, S. P. 2004, Nature, 430, 536
De Pontieu, B., Hansteen, V. H., Rouppe van der Voort, L., van Noort, M., & Carlsson, M. 2007, ApJ, 655, 624
Grossmann-Doerth, U., & Schmidt, W. 1992, A&A, 264, 236
Hale, G. E. 1908, ApJ, 28, 315
Hansteen, V. H., De Pontieu, B., Rouppe van der Voort, L., van Noort, M., & Carlsson, M. 2006, ApJ, 647, L73

Heggland, L., De Pontieu, B., & Hansteen, V. H. 2007, ApJ, 666, 1277
Heggland, L., Hansteen, V. H., De Pontieu, B., & Carlsson, M. 2011, ApJ, 743, 142
Langangen, Ø., Carlsson, M., Rouppe van der Voort, L., Hansteen, V., & De Pontieu, B. 2008, ApJ, 673, 1194
Leighton, R. B., Noyes, R. W., & Simon, G. W. 1962, ApJ, 135, 474
Lites, B. W. 1986, ApJ, 301, 992
Lites, B. W. 1992, in NATO Advanced Science Institutes (ASI) Series C, 375, eds. J. H. Thomas, & N. O. Weiss, 261
Rouppe van der Voort, L., & de la Cruz Rodríguez, J. 2013, ApJ, 776, 56
Rutten, R. J. 2012, Philosophical Transactions of the Royal Society of London Series A, 370, 3129
Stangalini, M., Giannattasio, F., Del Moro, D., & Berrilli, F. 2012, A&A, 539, L4
Suematsu, Y. 1990, in Lecture Notes in Physics, 367, Progress of Seismology of the Sun and Stars, eds. Y. Osaki, & H. Shibahashi, 211 (Berlin: Springer Verlag)
Suematsu, Y., Wang, H., & Zirin, H. 1995, ApJ, 450, 411
Tian, H., DeLuca, E., Reeves, K. K., et al. 2014, ApJ, 786, 137
Tsiropoula, G., Alissandrakis, C. E., & Schmieder, B. 1994, A&A, 290, 285
Vecchio, A., Cauzzi, G., & Reardon, K. P. 2009, A&A, 494, 269
Vissers, G., & Rouppe van der Voort, L. 2012, ApJ, 750, 22
Yurchyshyn, V., Abramenko, V., Kosovichev, A., & Goode, P. 2014, ApJ, 787, 58
Zhang, J., Tian, H., He, J., & Wang, L. 2017, ApJ, 838, 2